

https://dspace.org/

Solventless Isomerisation Reactions of Six-coordinate Complexes of Ruthenium and Molybdenum

Nareetsile, Florence Mmatshiamo

2006-11-14T06:29:26Z
http://hdl.handle.net/10539/1654

Downloaded from a DSpace repository. https://dspace.org/

CHAPTER 8

KINETIC STUDIES OF *cis*-$Mo(CO)_4(PPh_3)_2$ IN THE SOLID STATE

8.1 Introduction

The *cis*-$Mo(CO)_4(L)_2$ complex undergoes a *cis* to *trans* isomerisation reaction in solution [1] (see scheme below)

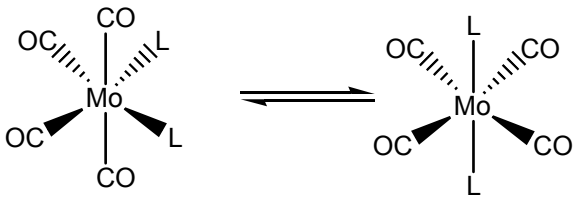

cis isomer *trans* isomer

Scheme 14 [refs 1 and 2]

Mechanistic studies on the *cis*→*trans* isomerisation process of $Mo(CO)_4(PPh_3)_2$ have revealed that this reaction involves initial dissociation of the PPh_3 ligand [2]. On the other hand for L = $P(^nBu)_3$ [3], PEt_3 [4] and PMe_3 [4] isomerisation to a *cis/trans* mixture occurs, without phosphine dissociation *i.e* isomerisation proceeds through an intramolecular pathway with the *trans* isomer being dominant.

cis-$Mo(CO)_4(L)_2$ complexes are reported to also undergo a ligand substitution reaction of one of the ligands L by carbon monoxide in solution [2, 5]. (See equation 8.1)

cis-$Mo(CO)_4(L)_2 + CO \rightarrow Mo(CO)_5L + L$ eq 8.1

This process has been observed to proceed via a dissociative mechanism (see scheme 15) [5]

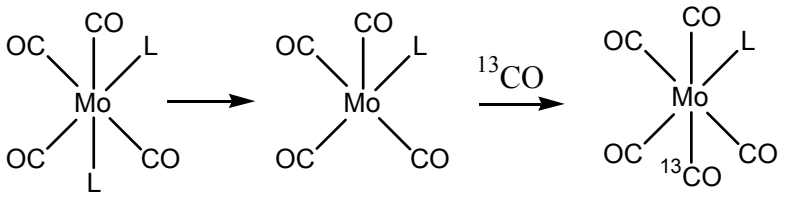

Scheme 15 [ref 2]

Thermal analysis studies of *cis*-$Mo(CO)_4(PPh_3)_2$ and *cis*-$Mo(CO)_4\{P(m\text{-tolyl})_3\}_2$ in chapter 7, revealed that they underwent isomerisation reactions in the solid state in the temperature range 120 ^oC to 160 ^oC while the other complexes *cis*-$Mo(CO)_4(PPh_2Me)_2$, *cis*-$Mo(CO)_4(PPh_2Et)_2$ and *cis*-$Mo(CO)_4[P(OEt)_3]_2$ isomerised in the melt. It was therefore decided to investigate the solid-state reactivity of the two Mo complexes (L= PPh_3 and P(*m*-tolyl)$_3$) in greater detail. The *cis*-$Mo(CO)_4(PPh_3)_2$ complex was chosen as a model to study the solid state isomerisation process because its solution chemistry and thermodynamic data is well documented [2]. Previous literature reports on solid state studies only focused on structural studies of this complex. Nothing has been mentioned in the literature about its reactions in the solid state.

This chapter describes kinetic studies of the solid state isomerisation reaction of *cis*-$Mo(CO)_4(PPh_3)_2$ monitored by two methods; a ^{31}P NMR spectroscopic method and a DRIFTS method. The findings of these two methods are reported in the subsequent sections.

8.2 DRIFTS

8.2.1 Historical perspective

In the literature, diffuse reflectance is also known as Kubelka-Munck reflection in honour of the two scientists that developed the theory of radiation transport in scattering media [6]. The technique was made possible by the advent of FTIR spectroscopy [7]. Diffuse reflectance is mostly used for studying powders and solids that have a rough surface [8]. Reflectance sampling techniques differ from transmission techniques in that the infrared

beam is bounced off the sample rather than passing through it [9]. Two fractions of radiation can be distinguished: one fraction is reflected from uneven areas of the rough surface; the other fraction penetrates the sample and is partially absorbed to be eventually scattered in the interior and return to the surface. The optical properties of a sample are then defined by its absorption and scattering coefficients in the Kubelka-Munk equation shown below

$$f(R_\infty) = (1-R_\infty)^2/2\ R_\infty + K/S$$

R_∞ is the degree of reflection on the sample surface at infinite thickness,
K is the absorption modulus and S the scattering modulus.

DRIFTS spectra are dependent on various sample preparation parameters as well as on geometric optical effects of the spectral measurement such that spectra of the same sample differ depending on the accessories used [10]. Parameters that are important in spectral acquisition include sample preparation method [11], particle size [12, 13], packing density [14, 15] and reaction mixture homogeneity [16]. It is critical that the above parameters are kept constant in investigations to obtain experimentally reproducible results.

The use of DRIFTS negates the need to press pellets such that sample preparation is simpler [17]. Also DRIFTS can be used to study a wide variety of samples other than samples dispersed in KBr pellets. The application of DRIFTS is widespread in the chemical industry. It has been used for the analysis of catalysts [18], in mechanistic studies [19], and for the characterisation of solid samples [20, 21]. The technique has also found use in forensic science [22, 23]. Quantitative analysis using DRIFTS has also been used for some time [24, 25].

8.2.2 DRIFTS in Organometallic chemistry studies

Diffuse Reflectance Infrared spectroscopy (DRIFTS) is an analytical tool that has been used in this thesis to investigate solventless reactions [26]. Like FTIRS, it was used to

detect reagents and products at very low concentrations [27]. The advantages that it has over FTIRS investigations of solventless reactions are that (i) it requires less sample per given reaction [28], (ii) the same sample can be used for a full experiment and many data points are generated per reaction so that it generates more accurate results and less experimental errors, (iii) there is no need to construct calibration curves, (iv) it takes less time to conduct an experiment and (v) the ability to work over a wide range of temperatures.

There are few other organometallic chemistry publications that have reported the use of this technique in the literature [29]. Examples include the study of the formation of chromogenic calyx[4]arene derivatives [30], a DRIFTS and NIR Raman investigation of supported and unsupported allyl-lanthanide complexes [31] and the reaction of molybdenum hexacarbonyl and benzene under thermal activation [32].

8.3 Experimental

The complex $Mo(CO)_4(PPh_3)_2$ was prepared as reported in chapter 7.

8.3.1 Kinetic studies by NMR spectroscopy

Kinetic studies were performed at constant temperature (in chosen temperature ranges) by heating *ca.* 10 mg of the solid sample in a sealed NMR tube for various time intervals. The NMR tubes containing the solid samples were evacuated and purged with nitrogen or CO prior to heating. After heating, the samples were cooled to room temperature and then dissolved in $CDCl_3$ and taken for ^{31}P NMR measurement. The % *ttt* isomer versus time curves for each individual isomerisation process was plotted (see Sections 8.4.1 and 8.4.2)

8.3.2 Kinetic studies by DRIFTS

DRIFTS experiments in this study were performed on a BRUCKER TENSOR 27 DRIFTS spectrometer. The instrumentation consists of an FT-IR spectrometer which houses the light source and the detector and a DRIFTS cell which contains a sample compartment.

The samples for DRIFTS studies were prepared by mechanical grinding of the complex, with previously dried KBr (diluent), to a very fine powder using a pestle and mortar. The materials were ground until a homogeneous mixture was obtained. A finely ground KBr powder was first loaded into a DRIFTS cell and measured as background. The homogeneous mixture of the complex in KBr (1 - 2%) was then loaded into the DRIFTS cell equipped with heating device, air and water inlet/outlets wirings (see figure 8.1). The initial IR spectrum was recorded (see figure 8.2). The heating control was then adjusted to the required temperature. The rate of disappearance of the peaks associated with the *cis*-isomer was measured by disappearance of the CO absorption peak at 2024 cm^{-1} (figure 8.3) until an appreciable amount of conversion to the *trans* isomer (figure 8.4) was achieved. A kinetic plot of the *cis*-isomer conversion (measured in terms of Kubelka Munck units) *versus* time was plotted (Section 8.4.5). Assuming that the reaction was 1st order, the Arrhenius plot for each individual isomerisation reaction was constructed. Samples were run under nitrogen. Kinetic plots were compared with equivalent reactions monitored by ^{31}P NMR spectroscopy (see above).

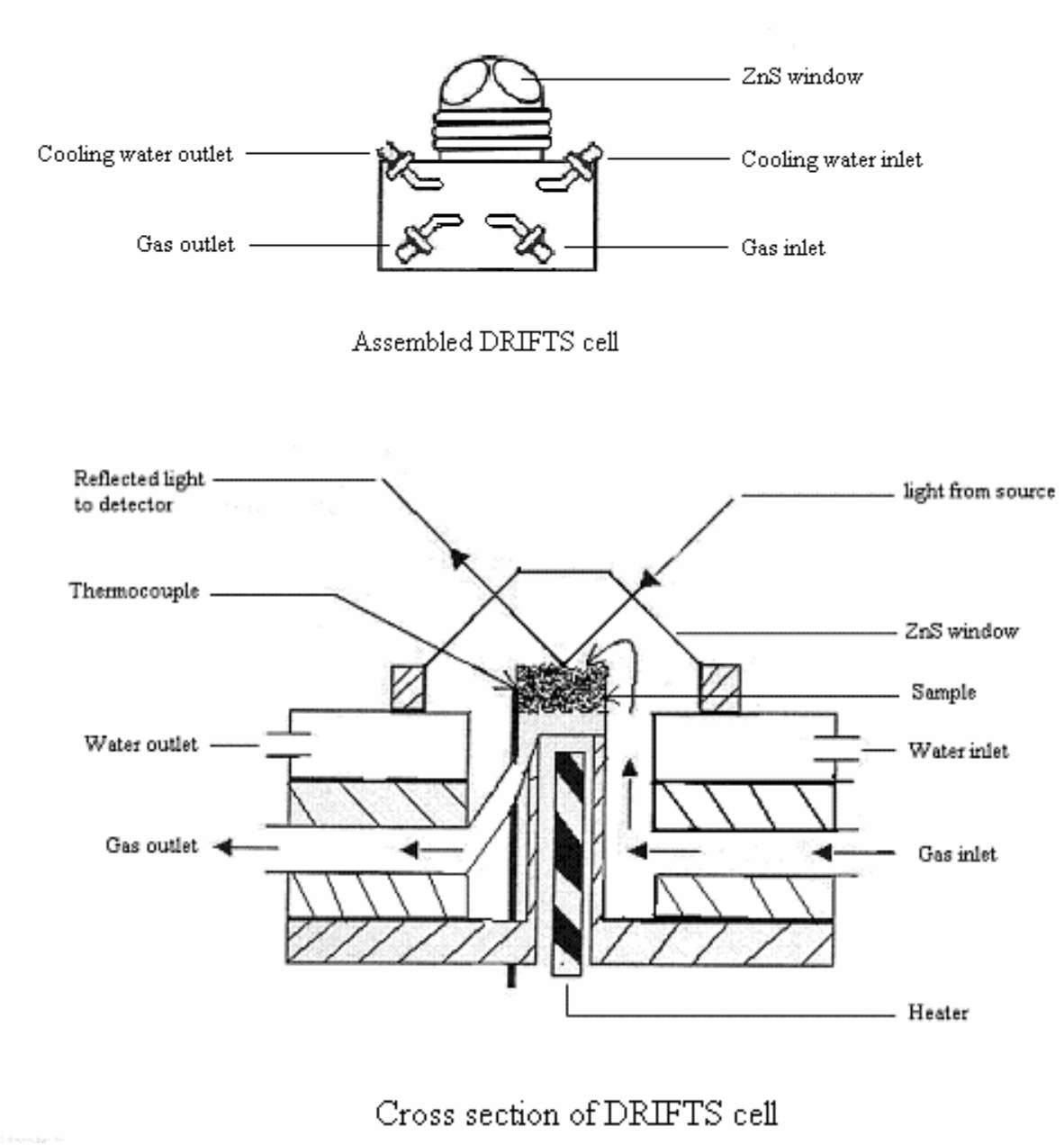

Figure 8.1: DRIFTS dome cell

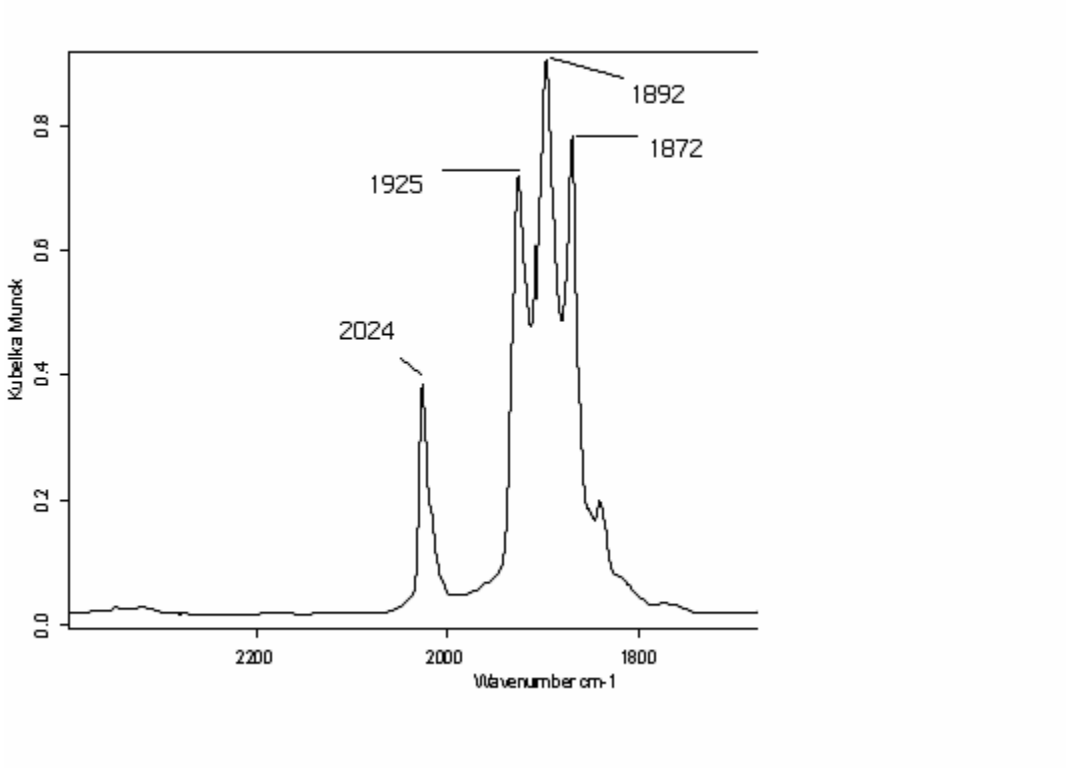

Figure 8.2: Initial IR spectrum of *cis*-$Mo(CO)_4(PPh_3)_2$ in the solid state at room temperature

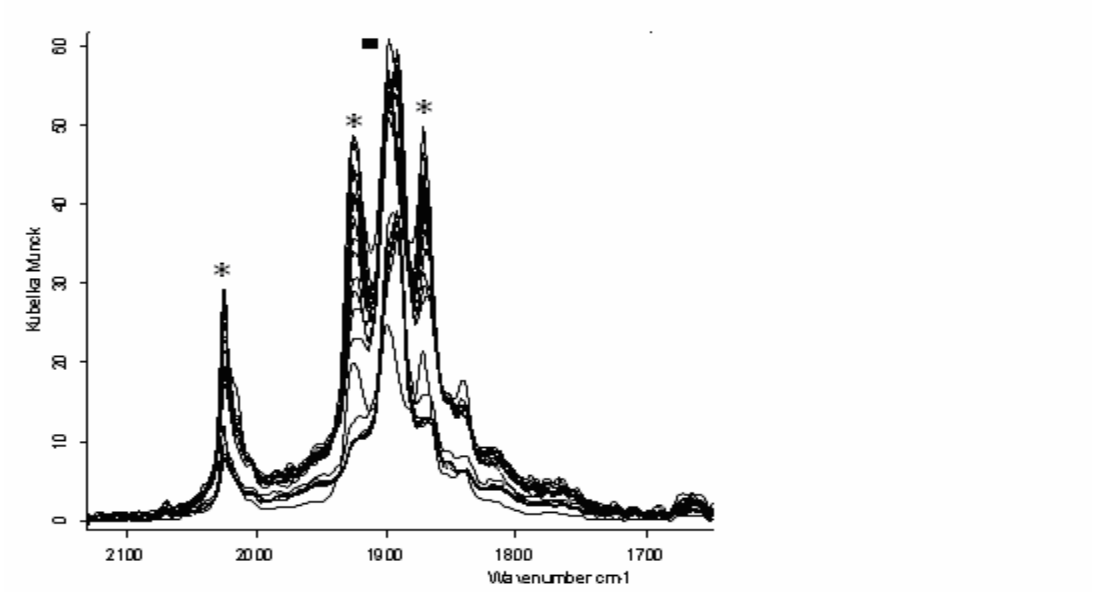

Figure 8.3: Disappearance of peaks due to *cis*-isomer (*) coupled with the appearance of peak due to the *trans*-isomer (■) during the reaction at 130 ^oC

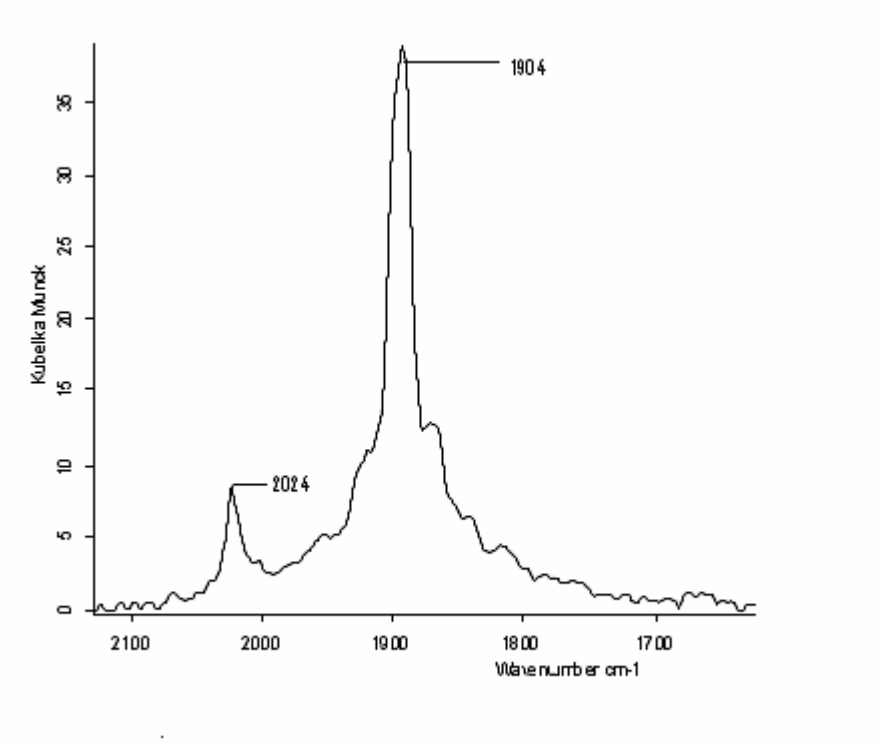

Figure 8.4: Resultant spectrum mainly of the *trans* isomer after heating of the *cis* isomer (130 ^{o}C).

8.4 Results and discussion

8.4.1 Isomerisation studies monitored by ^{31}P NMR spectroscopy (under nitrogen)

Plots of % *cis*-isomer versus time and that of lnα versus time at 120 ^{o}C were constructed (Figurews 8.5 and 8.6) for the isomerisation of *cis*-$Mo(CO)_4(PPh_3)_2$ to *trans*-$Mo(CO)_4(PPh_3)_2$. Plots of % *cis*-isomer versus time at 130 ^{o}C (figure 8.7) and 140 ^{o}C (figure 8.8) were also constructed. All the plots showed that the *cis* isomer converted to the *trans*- isomer with increasing time. The rate of conversion is also seen to increase with increasing temperature. The rate of conversion at 120 ^{o}C is very slow compared to the reaction performed at other temperatures. Data from higher temperatures (130 ^{o}C and 140 ^{o}C) seemed to follow first order kinetics and thus the isomerisation reaction of *cis*-

$Mo(CO)_4(PPh_3)_2$ was plotted as a first order reaction. However attempts to plot [ln α] (and other functions of α) versus time graphs yielded complex data which suggested that the reaction did not occur by first or other order reactions. An example of the [ln α] versus time plot is shown in figure 8.6. Part of the difficulty with attempting to plot the data is that in this procedure the generation of data is time consuming and leads to too few data points (each data point is a separate reaction). The inaccuracies in measurement overwhelmed the attempts at analysis. Similar studies were carried out on the data collected at 130 and 140 ^oC (not shown). Hence this approach to obtaining kinetic data was discontinued and DRIFTS (section 8.3.2) studies were rather undertaken.

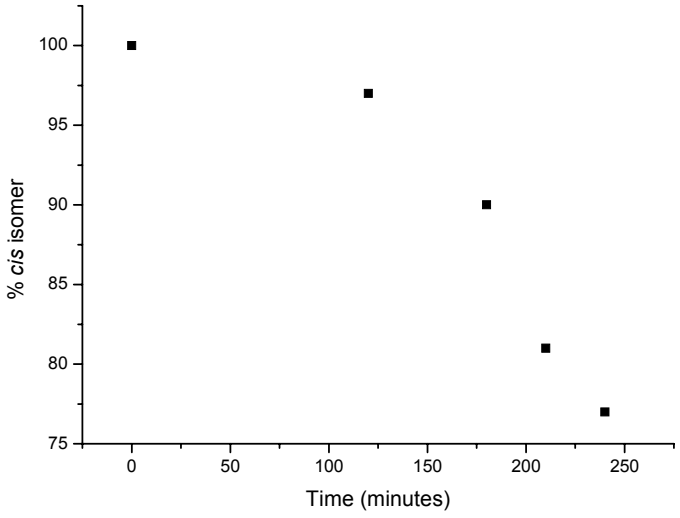

Figure 8.5: Thermal reaction of *cis*-$Mo(CO)_4(PPh_3)_2$ at 120 ^oC; Plot of % *cis*-isomer versus time

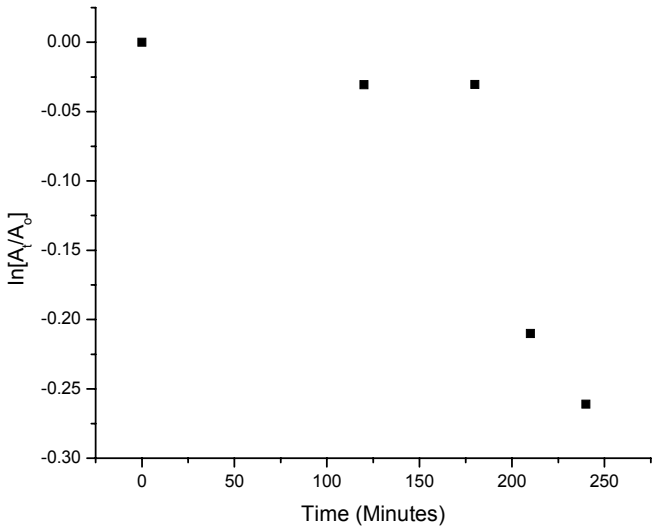

Figure 8.6: ln α versus time curve for *cis*-$Mo(CO)_4(PPh_3)_2$ at 120 ^oC

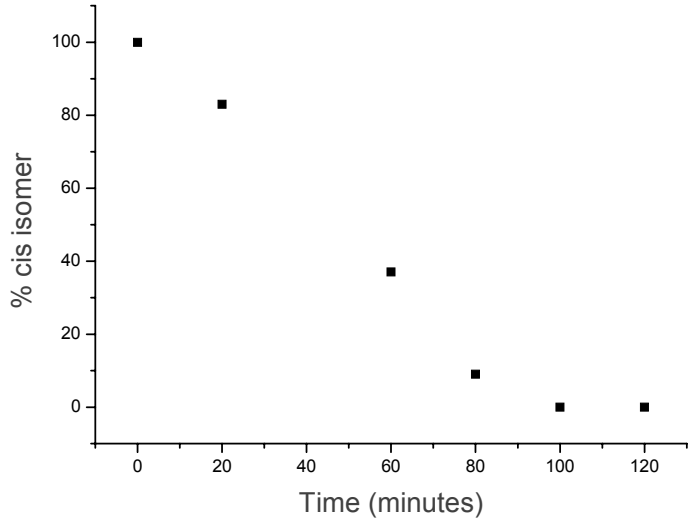

Figure 8.7: Thermal reaction of *cis*-$Mo(CO)_4(PPh_3)_2$ at 130 ^oC

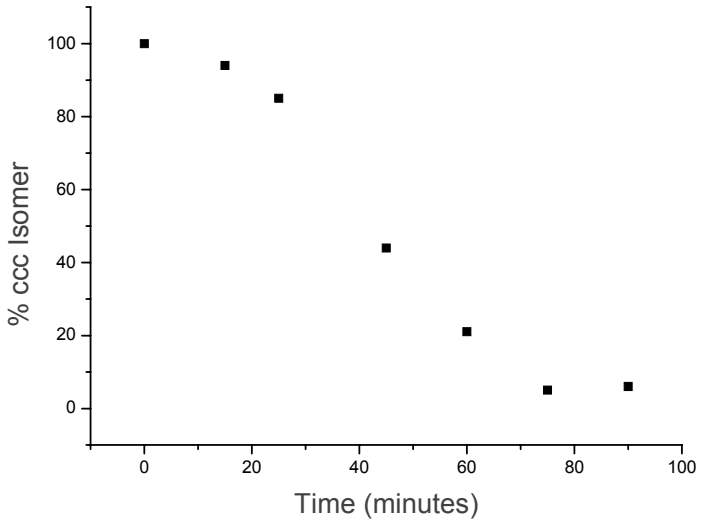

Figure 8.8: Thermal reaction of *cis*-$Mo(CO)_4(PPh_3)_2$ at 140 ^oC

8.4.2 Thermal reaction of *cis*-$Mo(CO)_4(PPh_3)_2$ under CO at various temperatures: analysis by ^{31}P NMR spectroscopy

The reactions were carried out to establish the effect of using CO instead of nitrogen gas on the reaction. The kinetic plot at 140 ^oC is shown in figure 8.9. It does show that the *cis*-isomer undergoes isomerisation when the heating time is increased. The isomerisation process is very slow. For example, under nitrogen after 180 minutes 100 % conversion was observed while under CO only a 48 % conversion was achieved. A ^{31}P NMR spectrum recorded on the reaction sample at the end of the reaction under CO does not show the presence of any oxidized phosphine. However, heating under nitrogen beyond 100 minutes gives complete conversion to the *trans* isomer and a significant amount of oxidised phosphine

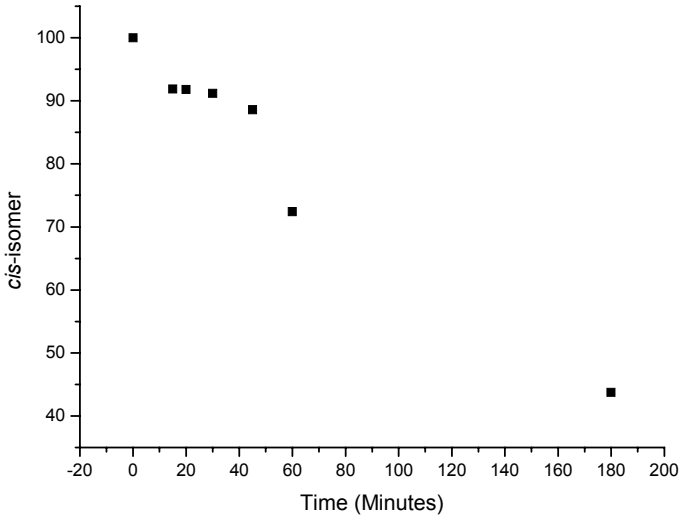

.

Figure 8.9: Thermal reaction of *cis*-$Mo(CO)_4(PPh_3)_2$ under CO at 140 ^oC

The kinetic plot at 150 ^oC is shown in Figure 8.10. The complex undergoes complete conversion to the *trans* isomer beyond 50 minutes (not shown). There is also the appearance of an oxidized phosphine peak in the NMR spectrum after 50 minutes which implies that the complex started decomposing before this time. Attempts to plot [lnα] versus time graphs did not yield a straight line implying either that the reaction was not first order or that the quality of the data collected by this technique are poor *e.g*. figure 8.11.

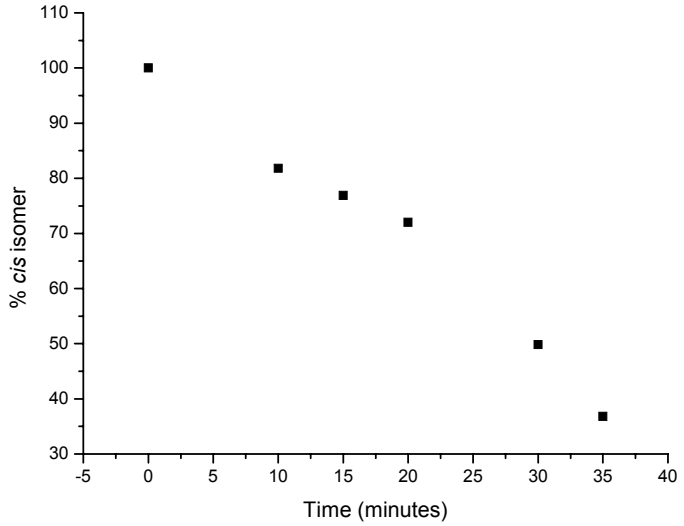

Figure 8.10: Thermal reaction of *cis*-$Mo(CO)_4(PPh_3)_2$ under CO at 150 ^oC

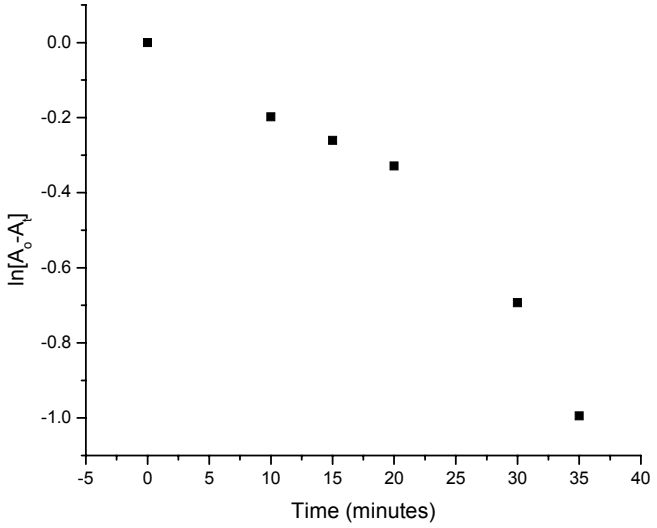

Figure 8.11: Plot of ln α versus time curve for thermal reaction of *cis*-$Mo(CO)_4(PPh_3)_2$ under CO at 150 ^oC

The kinetic plot at 160 ^oC is shown in figure 8.12. The plot reveals that after 20 minutes 80 % conversion to the *trans* isomer has occurred but that no phosphine oxide has appeared. However after 25 minutes (>90 % conversion) phosphine oxide can now be detected.

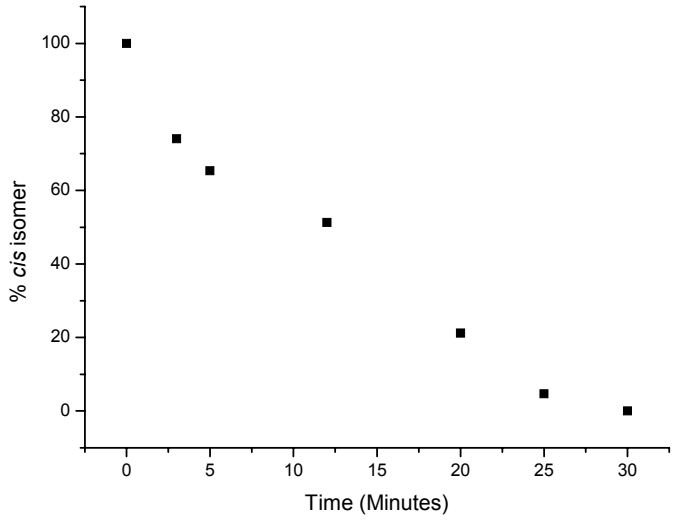

Figure 8.12: Thermal reaction of *cis*-$Mo(CO)_4(PPh_3)_2$ under CO at 160 ^oC

8.4.3 Effect of CO:

The presence of CO does affect the rate of the isomerisation process. When *cis*-$Mo(CO)_4(PPh_3)_2$ is heated at 140 ^oC under nitrogen for 60 minutes, there is 79 % conversion to the *trans* isomer, with the appearance of some oxidized PPh_3. When heated under CO at the same temperature there is only about 30 % conversion to the *trans*-isomer but no phosphine oxide is to be detected. The oxidised phosphine peak is only observed after 100 % conversion to the *trans* isomer. Therefore the CO not only affects the rate of the isomerisation reaction but it also seems to be taking part/playing a role in the reaction. Furthermore, $Mo(CO)_5PPh_3$ was detected in the reaction, even after 100 % conversion to the *trans* isomer under CO. In contrast, solution studies have indicated that CO displaces one PPh_3 ligand to give $Mo(CO)_5PPh_3$ when the reaction is carried out in solution under CO [2].

In the solid state, it appears that the oxidized peak associated with phosphine oxide comes from decomposed *trans* isomer since it does not appear in the early stages of the reaction and always appears after prolonged heating.

8.4.4 Colour changes noted during heating of *cis*-$Mo(CO)_4(PPh_3)_2$ under CO

On heating *cis*-$Mo(CO)_4(PPh_3)_2$ under CO in a sealed NMR tube , the colour of the complex gradually changes from dark yellow to pale yellow. The colour changes were noted by visual inspection. Samples which were heated for a long time gradually changed from pale yellow to orange and finally to dark green to a near black colour (for samples heated for a long time). The heated samples (black materials) were dissolved in chloroform after shaking for a long time. Samples heated beyond 40 minutes at 160 ^oC gave dark green solutions.

Dissolution of the samples obtained from heating experiments done at 140 and 150 ^oC under CO, showed the presence of PPh_3 (less than 1 %). This peak is detected in the early stages of the reaction and might arise when a minor amount of PPh_3 (not detected by IR spectroscopy) is displaced by CO. The PPh_3 was not observed for reactions done under nitrogen.

At 160 ^oC, no PPh_3 peak was detected but oxidised PPh_3 was observed towards completion of the reaction. This was also noted for reactions carried out at 140 and 150 ^oC. This suggests that the oxidized PPh_3 is a decomposition product obtained from the *trans* isomer. This peak was also observed after heating experiments under nitrogen. The question is: How does the PPh_3 get oxidised? There are two possible explanations; (i) it might be a decomposition product (ii) it might be obtained from a solution reaction occurring whilst collecting the NMR spectra of the samples.

Samples of both the *cis* and *trans* isomer were dissolved in chloroform to establish whether dissociation of the PPh_3 ligand occurred. It was observed that PPh_3 was detected whilst in solution *i.e* the oxidised phosphine ligand might have arisen from oxidation of the dissociated PPh_3 in solution during analysis of the samples.

8.4.5 DRIFTS studies of *cis*-$Mo(CO)_4(PPh_3)_2$ under nitrogen

DRIFTS studies were undertaken to evaluate the isomerisation reaction of *cis*-$Mo(CO)_4(PPh_3)_2$ under nitrogen. The following advantages have been observed when using DRIFTS compared to the NMR method discussed previously;

- DRIFTS allows for *in situ* measurements. In the NMR technique, one has to prepare different samples to obtain various points for a single kinetic plot, and hence a lot of sample is wasted whereas in DRIFTS only one sample is used and many points required for a single set of kinetic plot are obtained. Also, with the NMR technique, a lot of time is wasted in preparing the samples for heating and in measurement. Uniformity of the samples used for data points also brings in many complexities when measuring the kinetics of the reaction. With DRIFTS only one sample is used for all the data points and there is no problem with the uniformity of the samples.
- The reactions can be monitored in the solid state, whereas with the NMR technique, the samples have to be dissolved in solvents. Therefore, solvent effects might affect the kinetics of the reaction. Also the use of deuterated solvents and the use of many NMR tubes (for heating at various time intervals) is more expensive. Hence, DRIFTS is a cheaper technique than the procedure of monitoring the reaction by ^{31}P NMR spectroscopy.
- The ability to work in temperature range of 25 to 500 ^oC and to work under inert atmospheres

Data for the isomerisation reaction at 120 ^oC are shown in Figure 8.13. The isomerisation reaction appears to occur in three steps. The first step entails a slow reaction that occurs in less than 100 minutes. This reaction is likely to be described as an initiation step *e.g.* reaction occurring at a surface. This is followed by a rapid reaction between 100 and 300 minutes (propagation step), and a final slow reaction at 300 minutes and beyond (reaction approaching completion). This last reaction is very slow when compared to the first and second reaction rates. The data between 0 and beyond 800 minutes were re-plotted assuming that the reaction obeyed first order kinetics. In this time interval the kinetic

plot for product formation (trans isomer) using a product peak at 1477 cm^{-1} (which is also a peak due to *trans* isomer formation as previously shown in figure 8.3) gives a good first order plot (see figure 8.14).

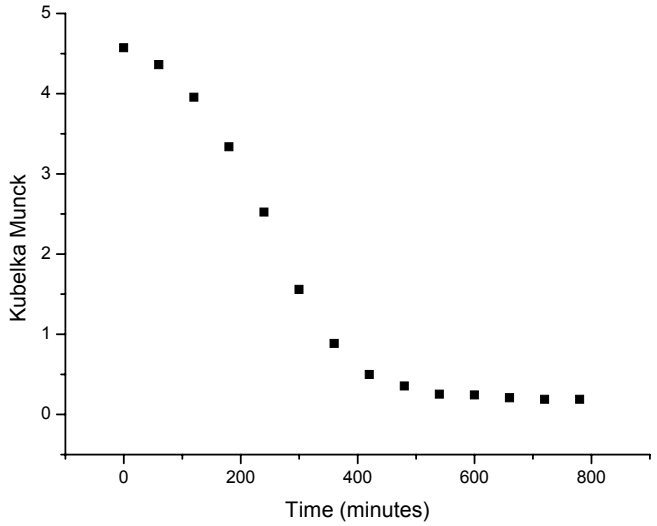

Figure 8.13: Kinetic plot of *cis*-$Mo(CO)_4(PPh_3)_2$ at 120 ^oC; data points collected at after 1 hr intervals

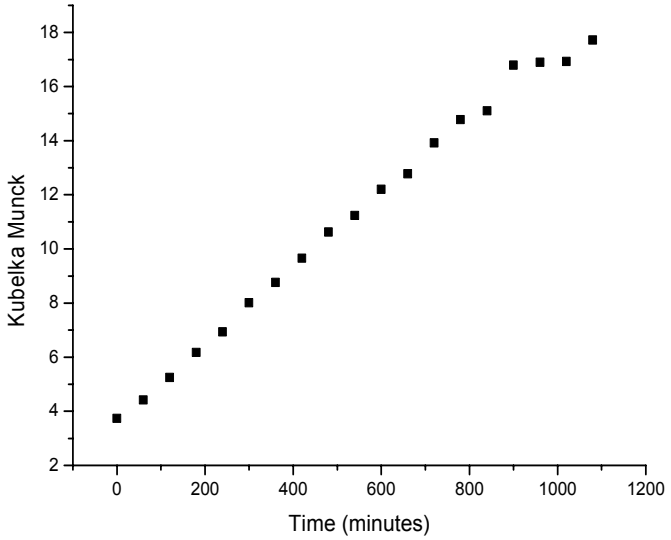

Figure 8.14: Kinetic plot for the formation of *trans*-$Mo(CO)_4(PPh_3)_2$ at 120 ^oC.

Reactions were also attempted at three other temperatures. At 130 and 140 ^{o}C (figures 8.15 to 8.18) the reaction is reasonably well behaved appearing to follow first order kinetics in the early stages of the reaction (first 100 minutes).

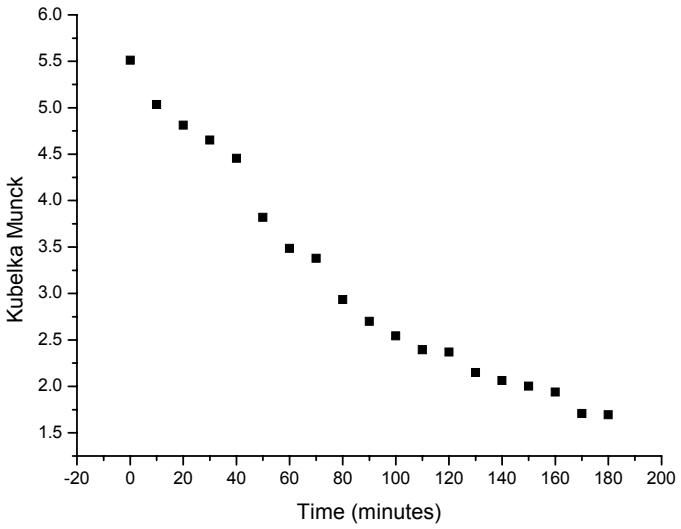

Figure 8.15: Kinetic plot of *cis*-$Mo(CO)_4(PPh_3)_2$ at 130 ^{o}C; data points collected after 5 minute intervals

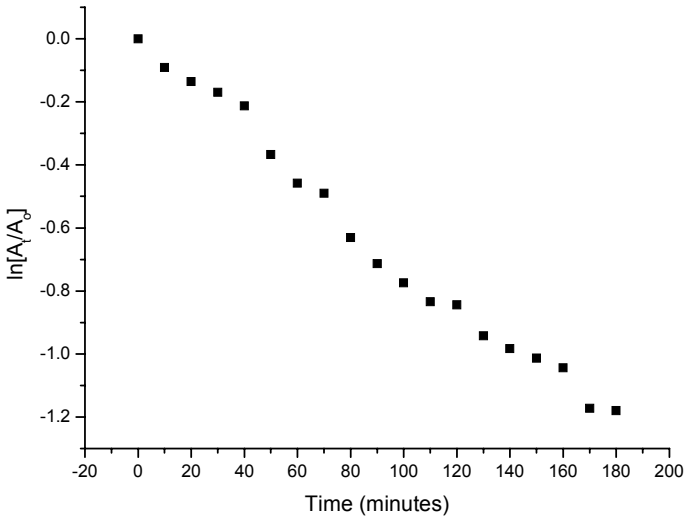

Figure 8.16: ln α versus time curve for the *cis*-$Mo(CO)_4(PPh_3)_2$ at 130 ^{o}C

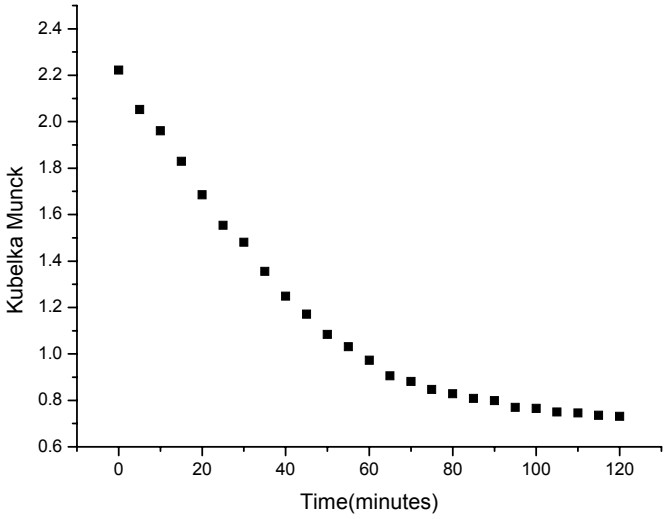

Figure 8.17: Absorbance versus time plot of *cis*-$Mo(CO)_4(PPh_3)_2$ at 140 ^oC; data points collected at 5 minute intervals.

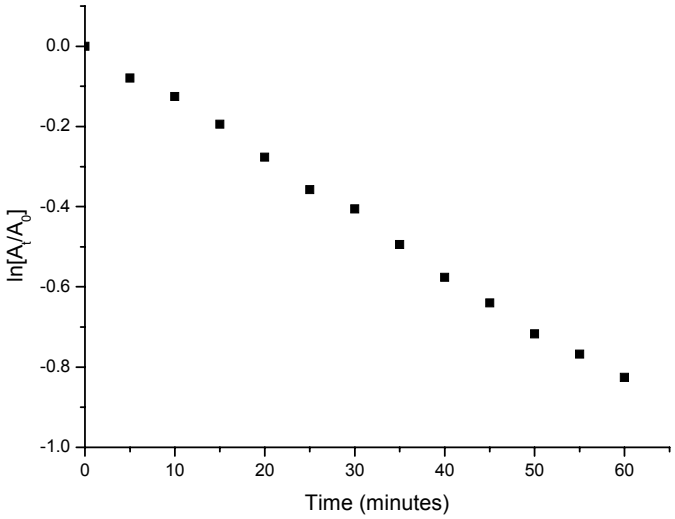

Figure 8.18: ln α versus time curve for the *cis*-$Mo(CO)_4(PPh_3)_2$ at 140 ^oC

The kinetic plots at 150 and 160 ^oC (figure 8.19 to 8.23) could also be replotted to fit a first order plot.

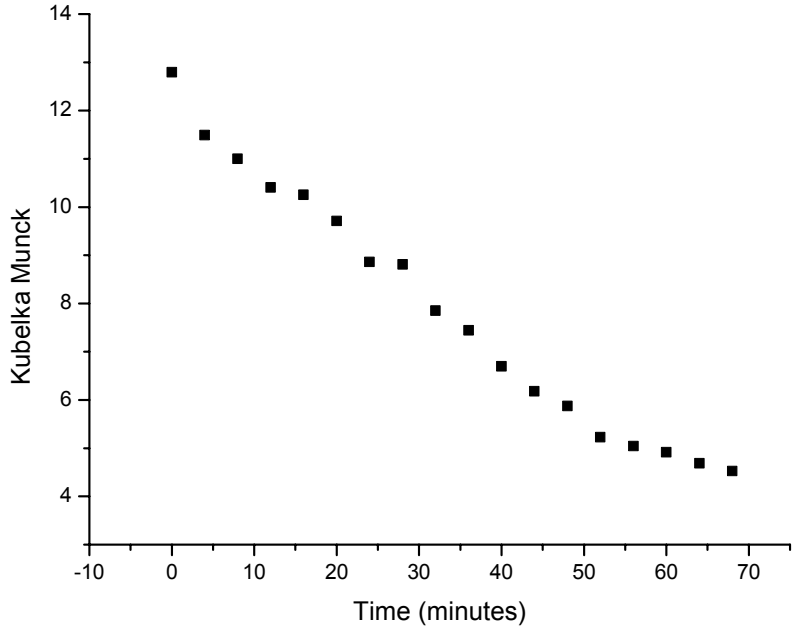

Figure 8.19: Thermal reaction of *cis*-$Mo(CO)_4(PPh_3)_2$ at 150 ^oC; data points collected at 4 minute intervals.

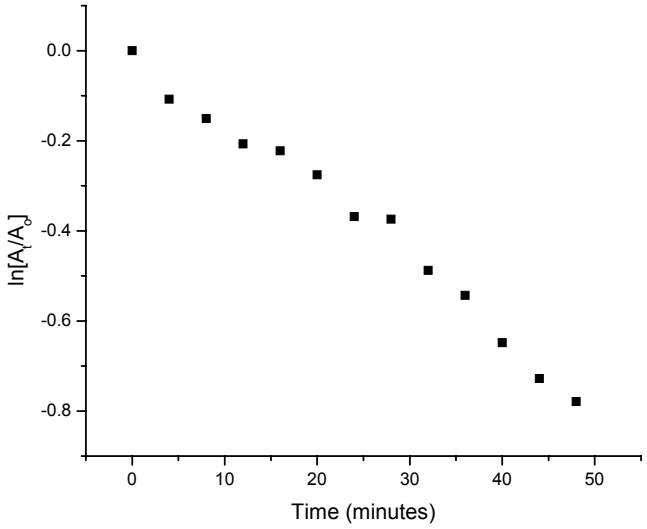

Figure 8.20: ln α versus time for the *cis*-$Mo(CO)_4(PPh_3)_2$ at 150 ^oC

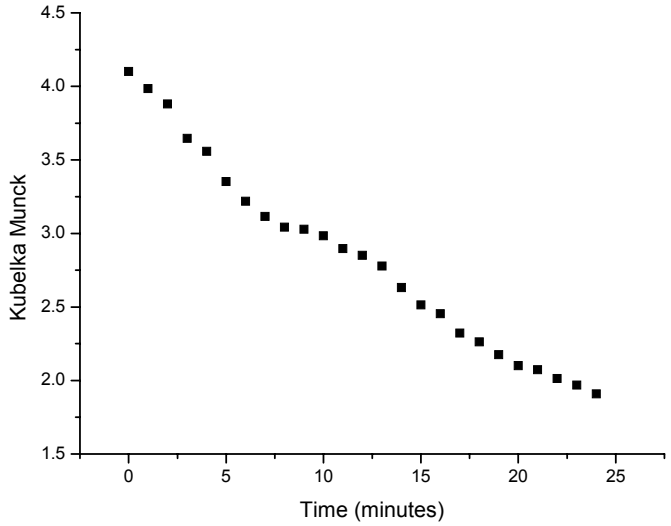

Figure 8.21 : Absorbance (Kubelka Munck) versus time plot of *cis*-$Mo(CO)_4(PPh_3)_2$ at 160 ^oC, data points collected at 1 minute intervals.

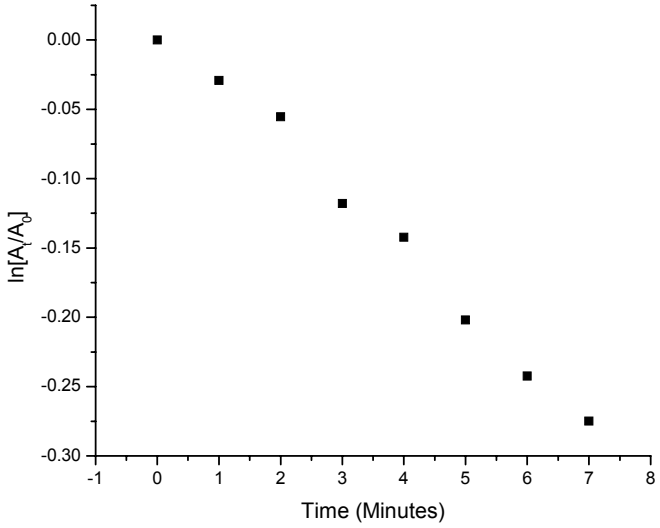

Figure 8.23: ln α versus time for the *cis*-$Mo(CO)_4(PPh_3)_2$ at 160 ^oC

Rate constants were obtained from the various temperature studies and the data are shown in Table 8.1.

Table 8.1: **Rate constants for isomerisation of the *cis*-$Mo(CO)_4(PPh_3)_2$ comlex at various temperature**

Temperature (^oC)	Rate constant , k (s^{-1})
130	$5.37 \pm 0.06 \times 10^{-3}$
140	$1.10 \pm 0.03 \times 10^{-2}$
150	$1.60 \pm 0.04 \times 10^{-2}$
160	$3.64 \pm 0.2 \times 10^{-2}$

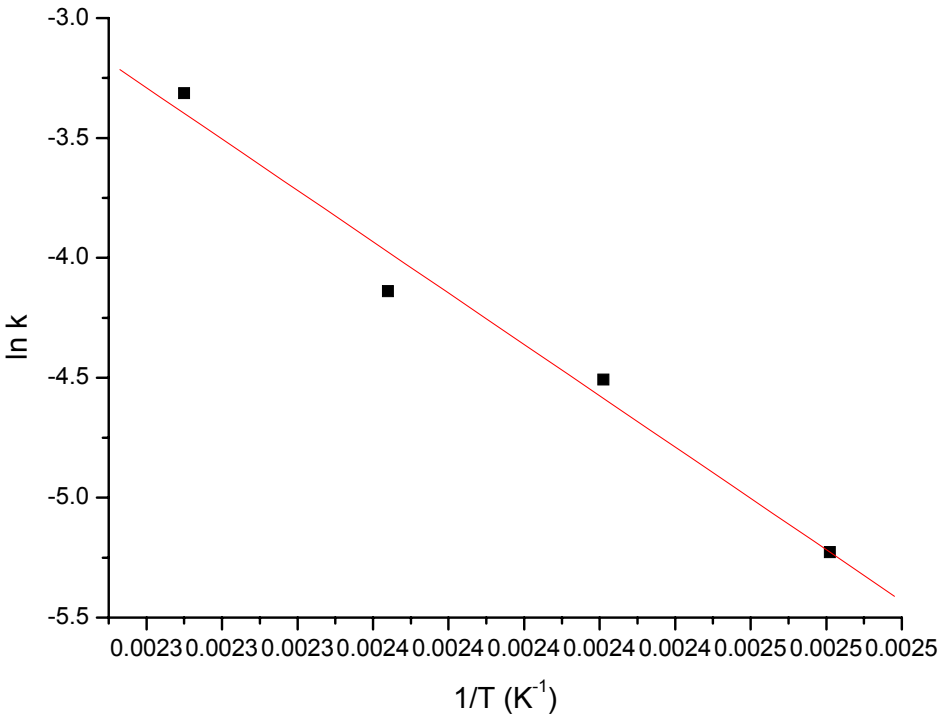

Figure 8.24: Arrhenius plot for *cis*-$Mo(CO)_2(PPh_3)_2$

An Arrhenius plot (figure 8.24) for the isomerisation of *cis*-$Mo(CO)_4(PPh_3)_2$ was constructed from k values collected at temperatures 130, 140 150 and 160 ^oC (see Table 8.1). The slope of the linear plot was found to be $-10702 \pm 1x10^2$ J $mol^{-1}s^{-1}$ and the calculated value of activation energy was found to be 89 ± 8 $kJmol^{-1}$.

8.4.6 Mechanism for the solid state reaction

Detailed studies have been undertaken on the *cis→trans* isomerisation reaction of $Mo(CO)_4L_2$ (L= PPh_3, PEt_3, $P(^nBu)_3$ and PMe_3) complexes in solution.

The solution data as mentioned in the introduction occur by either a *dissociative* or *intramolecula*r rearrangement.

The possible scenarios for the intramolecular reaction are shown in figure 8.25 [33].

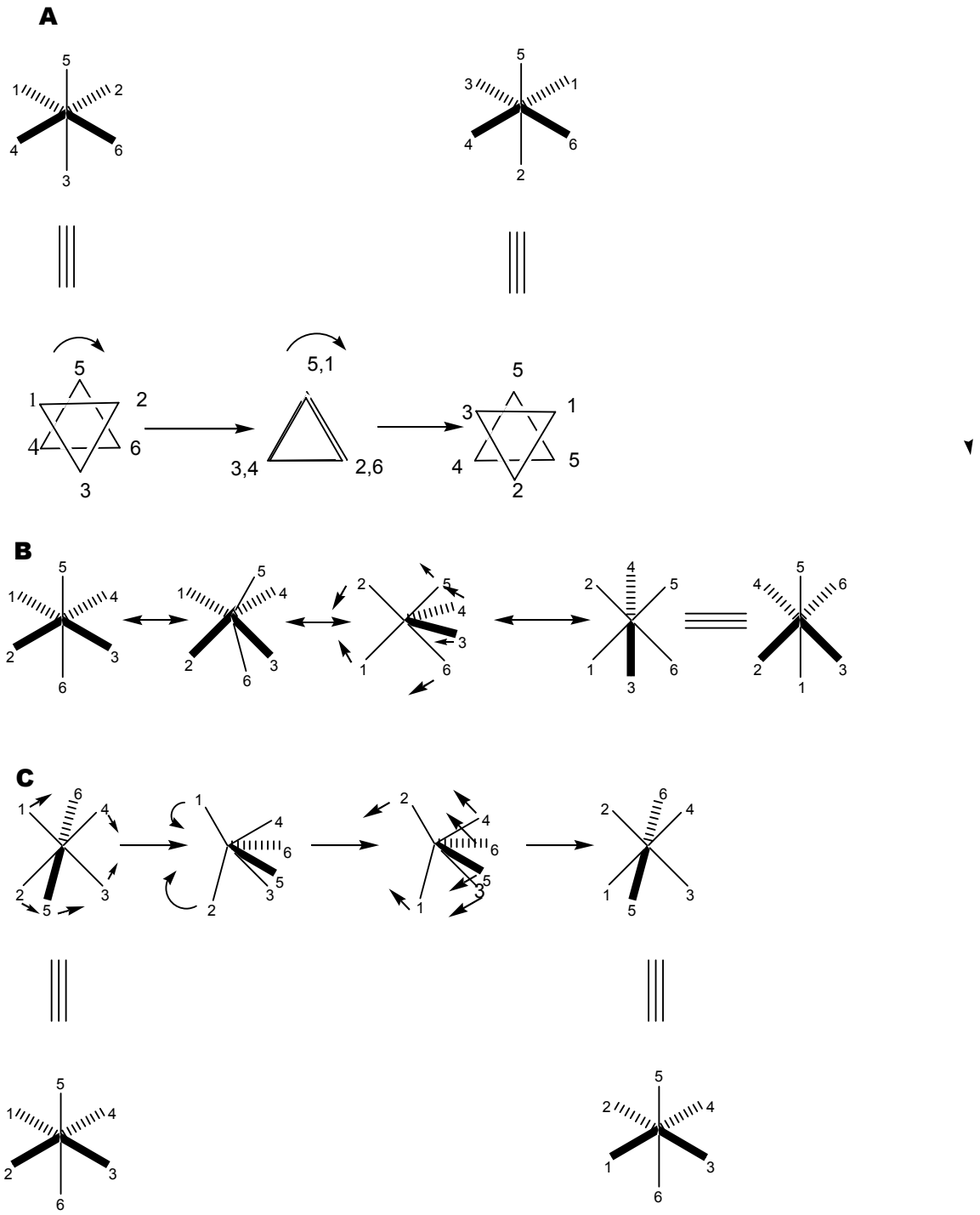

Figure 8.25: Isomerisation reaction mechanisms: A) through a trigonal prismatic intermediate B) through a bicapped-tetrahedra intermediate with a 90° rotation of the tetrahedral edge and C) through a bicapped-tetrahedral intermediate with a 180° rotation of the tetrahedral edge [33].

The solution studies revealed that data were consistent with mechanism A(*via* a trigonal prismatic intermediate). The data indicated that when L was large *e.g*. PPh_3 the dissociative process was the route used to isomerise the isomers.

The kinetic data obtained from the solid state reactions reveal the following;

(i) the reaction appears to go to completion (*cis* to *trans*)

(ii) Once formed the *trans* isomer decomposes at the high temperatures used in the kinetic study.

(iii) DRIFTS studies suggest that the reaction occurs *via* a first order process.

(iv) The Ea barrier is found to have values comparable to those found for dissociative and intramolecular studies in solution. Thus the value is consistent with either mechanism.

(v) No mixed phosphine/phosphite studies are possible in the solid state, ruling out this procedure for mechanism evaluation [33]

In the next chapter the results of an optical microscopy study of the reaction is reported. The key finding was the recognition that the reaction is a surface initiated process (Chapter 9).

The reaction involves movement of a large ligand (PPh_3) from a *cis* to a *trans* position. Data reveals that no CO ligand dissociate in the reaction (solution or solid state). Furthermore the reaction is inhibited by CO and no $Mo(CO)_5(PPh_3)$ is detected in the reaction.

This suggest that;

(i) the equilibrium $Mo(CO)_4(PPh_3)_2 \leftrightarrow Mo(CO)_4(PPh_3) + PPh_3$ lies far to the left and that

(ii) the intermediate in the reaction contains a weakened M-CO bond.

The issue then appears to be the degree to which rotation occurs without any bond breaking steps. A consideration of the mechanism involving a trigonal prismatic intermediate is shown in Scheme 16. The intermediate with the **L** group slowly interchanging with a CO ligand would be consistent with the data.

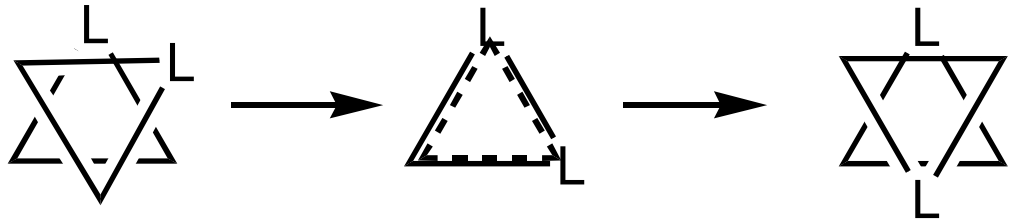

Scheme 16: L = PPh_3

The data are thus consistent with an *intramolecular* process but the possibility of PPh_3 dissociation cannot be totally discounted with the information at hand. What is clear is that the constraints of working in the solid phase have modified the reaction mechanism. In solution, dissociation of PPh_3 is facile but in the solid state the PPh_3 is constrained by the other reactant molecules. Clearly the constraint is significant- the reaction will be favoured at the surface where the large ligand can move. Once the isomerisation reaction is initiated the crystallinity is lost and more space now becomes available for further isomerisation.

The kinetic measurements are thus reflecting the movement of a 'reaction front' through the crystal- a reaction velocity directly associated with the isomerisation reaction.

8.5 Conclusion:

The kinetic studies of *cis*-$Mo(CO)_4(PPh_3)_2$ by NMR spectroscopy under nitrogen and carbon monoxide show that the isomerisation reaction occurs in the solid state in both cases, but the kinetic data from the NMR studies could not be used to evaluate the reaction mechanism. The data obtained on the isomerisation reaction monitored by DRIFTS revealed a first order reaction with Ea = 89 ± 8 $kJmol^{-1}$. A mechanism involving a trigonal prismatic intermediate has been proposed for the isomerisation of *cis*-$Mo(CO)_4(PPh_3)_2$ to the *trans* isomer in the solid state.

8.6 References

1 S. W. Kirtley, Comprehensive Organometallic Chemistry, vol 3, Chapter 27, Pergamon Press, Oxford.

2 D. J. Darensbourg, A. H. Graves, *Inorg Chem*. **18** (1979) 1257.

3 D. J. Darensbourg, *Inorg. Chem.* **18** (1979) 14.

4 F. A Cotton, D. J. Darensbourg; S. Klein, B. W. S. Kolthammer, *Inorg. Chem*. **21** (1982) 2661.

5 J. D. Atwood, Inorganic and Organometallic Reaction Mechanisms, Second Edition, Wiley-VCH.Chapter 4, p 95.

6 P. Kubelka, F. Munk, *Z. Techn. Phys*. **12** (1931) 593.

7 M. Fuller, P. Griffiths, *Anal. Chem*. **50** (1978) 1906.

8 H. Gunzler, H. Gremlich, IR Spectroscopy: An Introduction, Wiley-VCH Verlag, Weinheim, 2002.

9 B. C. Smith, Fourier Transform Infrared Spectroscopy, CRC Press, New York, 2000.

10 P. J. Brimmer and P. R. Griffiths, *Appl. Spectrosc*. **42** (1988) 242.

11 J. J. Benitez, M. A. Centeno, M. J. Capitan, J. A. Odriozolan, B. Viot, P. Verdier, Y. Laurent, *J. Mat. Chem.* **5** (1995) 1223.

12 O. Faix, J. H. Boettcher, *Holz als Roh-und Werkstoff* **50** (1992) 221.

13 Z. Krivacsy, J. Hlavay, *Spectrochim. Acta*. **50A** (1994) 49.

14 M. L. E. TeVrucht, P. R. Griffiths, *Appl. Spectrosc*., **43** (1989) 1492.

15 A. A. Christy, J. E. Tvedt, T. V. Karstand, R. A. Velapoldi, *Rev. Sci. Instrum.* **59** (1988) 423.

16 Y. K. Dijiba, A. Zhang, T. M. Niemczyk, *Int. J. Pharm.* **289** (2005) 39.

17 B. C. Smith, Infrared Spectral Intepretation: A Systematic Approach, CRC Press, Boca Raton, 1999.

18 J. Assmann, E. Loffler, A. Birkner, M. Muhler, *Catalysis Today* **85** (2003) 235.

19 N. Shirahama, S. H. Moon, K. –H. Choi, T. Enjoji, S. Kawano, Y. Korai, M. Tanoura, I. Mochida, *Carbon* **40** (2002) 2605.

20 R. J. Gordon, N. J. Trivedi, B. P. Singh, E. C. Ellis, *Environ. Sci. Technol.* **22** (1988) 672.

21 A. Kumar, G. C. Pandey, *Polym. Sci* **2** (1994) 911.

22 E. M. Suzuki, W. R. Gresham, *J. Forensic Sci.* **31** (1986) 931.

23 C. J. Lennard, W. D. Mazzella, P. A. Margot, *Analysis* **21** (1993) M34.

24 A. Tsuge, Y. Uwamino, T. Ishizuka, K. Suzuki, *Appl. Spectrosc.* **45** (1991) 1377.

25 G. C. Pandey, K. V. Rao, A. Kumar, *Polym. Testing* **14** (1995) 489.

26 S. S. Manzini, N. J. Coville, *Inorg. Chem. Comm*. **7** (2004) 676.

27 B. D. Chandler, L. H. Pignolet, *Catal. Today* **65** (2001) 39.

28 M. D. Bala, A. Budhai, N. J. Coville, *Organometallics* **23** (2004) 2048.

29 C. Bremard, *Coord. Chem. Rev.* **178** (1998) 1647.

30 I. Mohammed-Ziegler, *Spectrochim. Acta.* **59A** (2003) 3239.

31 H. Landmesser, H. Berndt, D. Kunath and B. Lucke, *J. Mol.Catal. A* **162** (2000) 257.

32 C. Bremard, G. Ginestet, M. Le Maire, *J. Am. Chem. Soc.* **118** (1996) 12724.

33 A. A. Ismail, F. Sauriol, I. S. Butler, *Inorg. Chem*. **28** (1989) 1007.